

TOPOLOGICAL ANALYSIS OF HIGH-RESOLUTION CMB MAPS ^a

B.D. WANDEL, E. HIVON, K.M. GORSKI,
*Theoretical Astrophysics Centre (TAC), Juliane Maries Vej 30,
 2100 Copenhagen Ø, Denmark*

We report the development of numerical tools for the topological analysis of sub-degree resolution, all-sky maps. Software to be released in the HEALFAST (V0.9) package defines neighbour relationships for the HEALPIX tessellation of the sphere. We apply this routine to a fast extrema search which scales strictly linearly in the number of pixels, N_p . We also present a highly efficient algorithm for simulating the gradient vector and curvature tensor fields “on-the-fly” with the temperature map, needing only of order $N_p \log_2 N_p$ more operations.

1 Introduction

The Microwave Anisotropy Probe (MAP) and the Planck Surveyor satellite missions promise to produce high-resolution full sky maps of the Cosmic Microwave Background (CMB) within the next decade. These maps will contain a great deal of cosmologically relevant information and therefore present a tremendous opportunity for doing high-precision cosmology. Owing to the unprecedented wealth of data, this opportunity brings with it the challenge of developing tools which help extract this information in manageable processing time.

Much attention has been given to the problem of estimating the angular power-spectrum of CMB anisotropies. To illustrate the difficulties one is facing, we note that even choosing the fastest presently available algorithm and allowing for parallelisation and technological advance, the estimation of the angular power-spectrum C_l of CMB anisotropies will take $\gtrsim 6$ years¹ for future million pixel maps.

While the C_l spectrum is the statistic of choice for a large class of cosmological models where the primordial fluctuations are Gaussian distributed, the possibility remains that another physical mechanism produced structure in the universe. In this case the CMB maps will almost certainly be non-Gaussian and contain more information than merely the power on different angular scales. Failing this, non-linear gravitational effects and foregrounds will produce detectable non-Gaussian signals.

Even for Gaussian maps, it has been shown that extrema statistics capture information about cosmological parameters and their theory is well developed^{2,3,4,5}. The importance of studying these and other topological properties of CMB temperature and polarisation has been noted by several authors⁶. Extrema have the advantage that they dominate the noise and are therefore very robust. As a consequence they have been among the first scientific results reported from recent CMB observations (one of them even at this conference⁷!).

The aim of this talk is to present tools which allow the implementation of a wide range of data analysis and processing techniques on the sphere.

^aFull size, full colour images can be downloaded from <http://www.tac.dk/~wandelt>

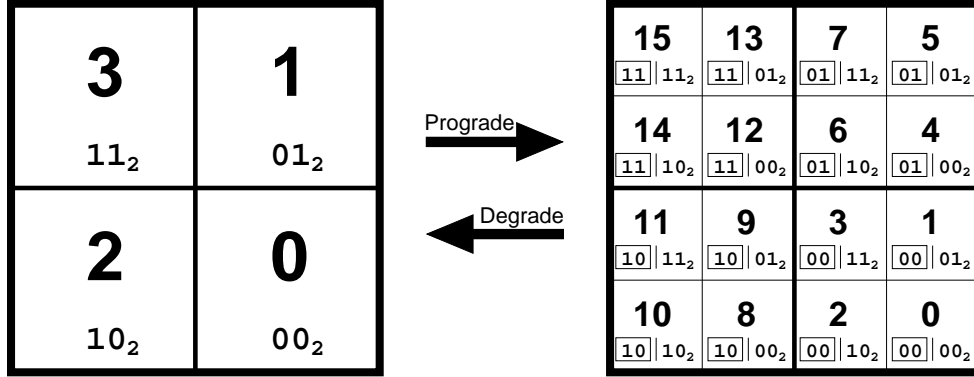


Figure 1: Quadtree pixel numbering. The coarsely pixelised coordinate patch on the left consists of four pixels. Two bits suffice to label the pixels. To increase the resolution, every pixel splits into 4 daughter pixels shown on the right. These daughters inherit the pixel number of their parent (boxed) and acquire two new bits to give the new pixel number. Several such coordinate patches are joined at the boundaries to cover the sphere. All pixels carry a prefix (here omitted for clarity) which identifies which patch they belong to.

2 Tools

2.1 Neighbour relationships on the sphere

Finding neighbours of a given pixel is essential for performing many local operations on digitised data, such as finding extrema, saddle points and zero crossings, finite differencing, extraction of patches, real-space filtering *etc.* While next-neighbour relationships are trivially defined on a lattice in the plane, on the sphere it is necessary to match distinct coordinate patches. Further, in a spherical topology the number of next-neighbours is not the same for all pixels.

We base our methods on the HEALPIX tessellation of the sphere⁸. However, even when a pixelisation of the sphere is given, we must still decide how to number the pixels. We choose the hierarchical, quadtree numbering scheme illustrated in Figure 1. This scheme is well-known and was used for the COBE pixelisation. Its main advantages for finding next-neighbours are that

- a neighbour can be found by direct operation on the binary representation of the pixel number which is computationally very cheap (finding all next-neighbours of 12×10^6 pixels takes less than 10 seconds^b);
- the algorithm is manifestly resolution independent owing to the self-similarity of the numbering scheme;
- once an algorithm exists that finds next-neighbours, it can easily be extended to find a whole neighbourhood of a pixel by first degrading, then finding next-neighbours and then prograding.

A disadvantage is that in its implementation the boundary matching of coordinate patches has to be customised for the chosen pixelisation scheme. But even here the symmetries of the quadtree are useful. For example, if two patches like the one on the right of Figure 1 were joined side by side, neighbours of pixels at the joining edge can be found by inverting all even bits of their pixel number, *e.g.*, $4 = \underline{0}1\underline{0}0_2 \leftrightarrow 14 = \underline{1}1\underline{1}0_2$. This and analogous prescriptions generalise to arbitrary resolution.

As an example application, we show in Figure 2 the theoretical prediction and our numerical results for an extrema search in a “standard” CDM and an open model with $\Omega = 0.2$ ($H_0 =$

^bAll timings are “wall clock” for a single SGI R10000 194MHz processor.

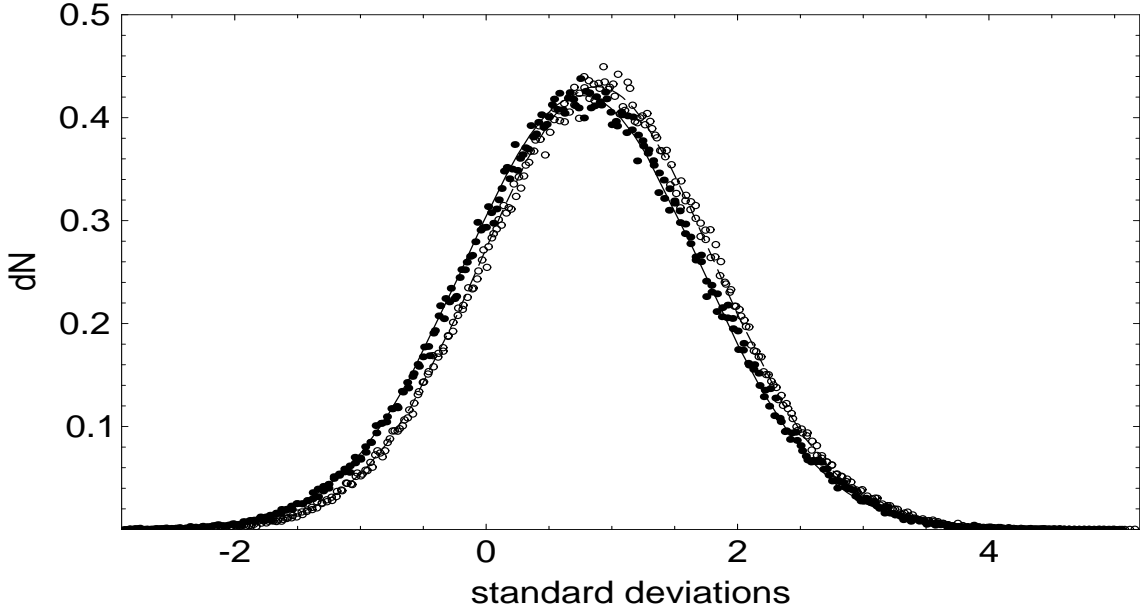


Figure 2: Probability density for finding a maximum (minimum) above (below) a certain excursion level. The minima distributions have been flipped over to coincide with the maxima distributions. Open dots are found from one realization of an $\Omega = .2$ map, filled dots are for standard CDM. Lines show the theoretically expected distributions (solid: SCDM, dashed: OCDM).

50km/s/Mpc, $\Omega_b = 0.05$ for both, $\theta_{FWHM} = 10'$ and zero noise). While it is clear that these probability distributions contain much less information than the anisotropy spectrum (they form a 3 parameter family if the total number of pixels is counted), the distributions shown clearly distinguish the two models. We stress that this is a realistic situation, since we used data only from one map.

This example do not even begin to explore the possibilities of these methods. By just measuring the probability distribution of excursion of an extremum from the mean, we are throwing away valuable scale and phase information. A more careful analysis will reveal more about the specific advantages of topological analyses of CMB maps.

2.2 Map simulation and computation of derivative fields

The derivative fields of a map are important for the study of the properties of its stationary points. A Fast Spherical Harmonics Transform code exists for the synthesis of Gaussian HEALPIX temperature maps with a given C_l spectrum⁹. A priori, generating the derivative fields would take just as long for each component as the map generation itself. The time limiting factor for map generation is the calculation of the associated Legendre polynomials $P_l^m(\cos \theta)$ for each ring of constant co-latitude θ . We exploit this fact by calculating the derivative fields at the same time as the temperature map and exploiting the following differential relations:

$$\begin{aligned}
 \frac{\partial}{\partial \phi} Y_{lm}(\theta, \phi) &= im Y_{lm}(\theta, \phi) \\
 \frac{\partial}{\partial \theta} Y_{lm}(\theta, \phi) &= -m \cot \theta Y_{lm}(\theta, \phi) - \sqrt{l(l+1) - m(m-1)} Y_{l, m-1}(\theta, \phi) e^{i\phi} \\
 \frac{\partial^2}{\partial \theta^2} Y_{lm}(\theta, \phi) &= - \left(\left[l(l+1) - \frac{m^2}{\sin^2 \theta} \right] + \cot \theta \frac{\partial}{\partial \theta} \right) Y_{lm}(\theta, \phi)
 \end{aligned} \tag{1}$$

In this way, only five more Fast Fourier Transforms have to be computed for each ring on the sphere, with the total added cost scaling as $N_p \log_2 N_p$. For a map with $N_p = 12.6 \times 10^6$ pixels, this amounts to an added 15 minutes of wall clock computation time for all five derivative components compared with 20 minutes for the temperature alone. In Figure 3 we display temperature anisotropies, the square norm of the gradient vector $|\nabla_i T|^2 = \frac{1}{\sin^2 \theta} \left(\frac{\partial}{\partial \phi} T \right)^2 + \left(\frac{\partial}{\partial \theta} T \right)^2$ and the trace of the curvature tensor $\text{Tr}(\lambda_{ij}) = \frac{1}{\sin^2 \theta} \frac{\partial^2}{\partial \phi^2} T + \frac{\partial^2}{\partial \theta^2} T$, for the standard CDM model.

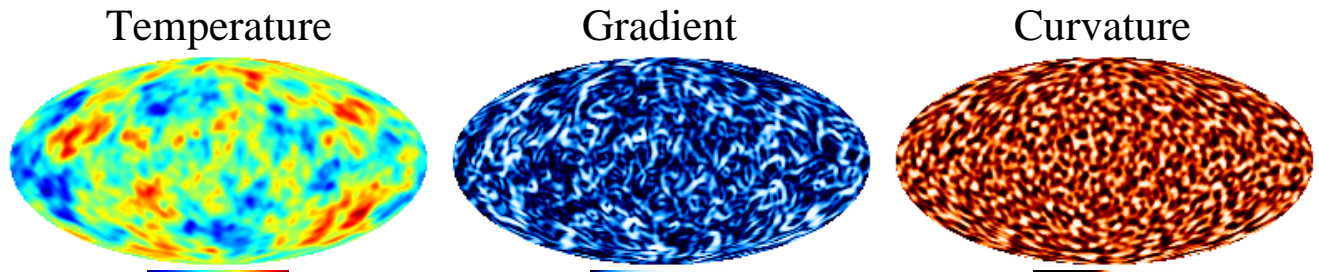


Figure 3: From left to right: the temperature, the square of the gradient vector and the trace of the curvature tensor for a standard CDM sky smoothed at 5 degrees for easier visualisation.

3 Conclusions

In this talk we presented tools which are generally applicable for the analysis of topological properties of maps on the sphere such as the detection of extrema, saddle points and zero crossings of a function, even though they can be used more generally for any kind of local analysis of spherical data sets. The computational time required for all sky computations scales strictly as the number of pixels in the map, N_p . Further, we extend existing simulation tools for Gaussian fields to generate not only temperature maps but also the associated gradient vector and the curvature tensor fields, with the extra computational cost scaling as $N_p \log_2 N_p$.

Acknowledgments

This work was supported by Dansk Grundforskningsfond through its funding for TAC.

References

1. J. Borrill, preprint, astro-ph/9712121.
2. M. Sazhin, *M.N.R.A.S.* **216**, 25P (1985).
3. J.R. Bond and G. Efstathiou, *M.N.R.A.S.* **226**, 655 (1987).
4. N. Vittorio and R. Juszkiewicz, *Ap. J.* **314**, L29 (1987).
5. R.B. Barreiro *et al.*, *Ap. J.* **478**, 1 (1997).
6. M. Sazhin and Toporenskii *Astr. Lett.* **22**, 791 (1996); P. Arbuzov *et al.*, *Int. J. Mod. Phys. D* **6**, 409 (1997); P. Arbuzov *et al.*, *Int. J. Mod. Phys. D* **6**, 515 (1997); P.D. Naselsky and D.I. Novikov, preprint, astro-ph/9801285.
7. J. Baker, in this volume.
8. K.M. Gorski, in preparation.
9. E. Hivon and K.M. Gorski, in preparation.